Proceedings Paper:
Oloyede, O, Biggs, T and Mullis, A (2015) Characterization of rapidly solidified commercial grey cast iron in drop-tube. In: Materials Science and Technology Conference and Exhibition 2015, MS and T 2015. Materials Science and Technology Conference and Exhibition 2015, 04-08 Oct 2015, Columbus, Ohio, USA. Association for Iron and Steel Technology , pp. 843-849. ISBN 9781510813939

CHARACTERIZATION OF RAPIDLY SOLIDIFIED COMMERCIAL GREY CAST IRON IN DROP-TUBE

Olamilekan Oloyede[1,2]; Tim Biggs[1]; Andrew Mullis[1]

[1]Institute for Materials Research, The University of Leeds, LS2 9JT Leeds, United Kingdom

[2]School of Marine Engineering, Maritime Academy, Nigeria. engrlekanoloyede@yahoo.com

Keywords: Rapid Solidification, Grey Cast Iron, Microstructure, Drop-tube, Cooling rate

Abstract

This study presents containerless solidification of BS1452 grade 250 commercial grey cast iron using 6.5m drop-tube apparatus. It gives a comparative summary of microstructural changes that occur between the rapidly cooled droplet particles as against its conventional slowly cooled control as-cast sample. The bulk as-received sample was melted and rapidly cooled during free fall in high vacuum containerless equipment. These rapidly solidified samples were collected and sieved into size ranges from >850 μm to <53 μm diameter, corresponding to estimated cooling rate of 500 K s^{-1} to 75,000 K s^{-1} with each sieve fraction being prepared for metallographic characterization. The analytical methods used include; light optical microscope and scanning electron microscopy, x-ray diffraction and differential thermal analyses. The result of this investigation reveals that the microstructure of the as-cast sample shows flake graphite randomly dispersed in ferrite matrix which is typical of slowly cooled grey cast iron. In contrast, flake graphite was absent in virtually all drop-tube samples even those with modest cooling rate. The evolved microstructure clearly shows the effect of cooling rate on the transformation from the conventional to rapidly solidified droplet particles in terms of microsegregation.

Introduction

Evidence abound in the metallurgical community that solidification processing affects microstructure and mechanical properties which in turn affect materials' performance. Many researchers are now more interested in rapid solidification technology as a means of re-engineering or manipulating materials microstructure to influence their inherent property for better output while in use. Using a typical containerless solidification method, a number of microstructural evolutions and discoveries have been revealed in several different metallic and alloy systems, due to increasing undercooling which has led to many noticeable phase transformations and refinement in both ferrous and non-ferrous alloys [1-3].

Containerless processing is an effective tool for undercooling metallic liquid far below their equilibrium melting temperatures. Generally, processes involving rapid solidification of alloys have a great practical potential of doing one or more of totally re-orientating microstructure, possible extended solid solubilities, microsegregation-free crystal or retainment of metastable phases and better chemical homogeneity which can be obtained at high cooling rates [4]. Drop tube, electromagnetic levitation, acoustic levitation and gas atomization are all containerless solidification methods which are used to obtain high melt undercooling of alloys. By using these methods under clean environmental conditions, the

dominant heterogeneous nucleation on container walls and free surfaces will be completely eliminated. An inert environment is normally provided by high vacuum in order to prevent any kind of disadvantageous effect such as oxidation [5]. Literally, the end effect of these non-equilibrium solidification methods on the evolved microstructures of the produced powders can be easily ascertained with standard microhardness measurement to affirm its relationship with droplets size and cooling rate.

Among all these containerless rapid solidification processing methods, drop tube technique stands out for large production of different size rage of metallic droplets and it is very suitable for nucleation and microstructure investigations in spherical or near spherical droplets. Drop-tubes are categorized as long or short according to the tube heights. Long drop tubes are generally >50 m in height and it is commonly used to process one individual droplet at a time; while short drop tubes process a spray of droplets of various size groups. Relevant literature survey shows that there are quite many drop tube system of different heights in existence such as 2.5 m [6], 3 m [7], 6.5 m [8, 9], 8 m [10], 14 m [11], 26 m [12], 32 m [13], 47 m [14], 100 m [15], 105 m [16], all these offer containerless solidification conditions. Drop tube technique provides microgravity conditions to the melt particles falling in the tube, which affects nucleation and heat transfer during solidification process.

Experimental procedure

The material used for this study was grey cast iron which remains the most casting materials with over 6 million of the total world's production tonnage [17]. Conventionally solidified low alloyed commercial grey cast iron specification BS 1452 Grade 250 was supplied as continuous 25 mm x 60 mm round bar by West Yorkshire Steel, United Kingdom. Table I confirms the compositional analysis obtained for the alloys. The droplet samples were obtained using 6.5 m high drop-tube facility in the Institute for Materials Research, University of Leeds. The droplets were sieved into 9 different standard groups ranging from ≥ 850 μm to ≤ 53 μm powder sizes. These were then hot mounted along with as-cast sample for metallography, examination and analysis. The microstructure of the sample were examined using light optical microscope and scanning electron microscopy (SEM) with in-built energy dispersive x-ray diffraction (XRD) analysis using Cu Kα radiation at room temperature.

Result and Discussion

Figure 1a shows the bulk as received clean sample of the supplied grey cast iron bar from which smaller pieces shown in figure 1b were cut-out to produce powder droplets from drop-tube processing. The micrographs of this and the resulting rapidly solidified particles sizes are thereafter discussed in relation to their emergent morphologies, microstructure and phase transformation as a result of rapid solidification of the droplets as compared to the as-cast.

a

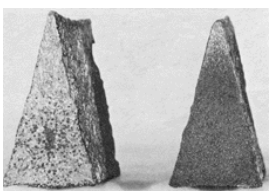

b

Figure 1: (a) Bar and (b) pieces of as-cast commercial BS1452 Grade 250 Gray cast iron.

Table I: Elemental composition of commercial grey cast iron BS1452 grade 250 as analyzed using XRF as compared to that obtained from EDX analysis using LEMAS SEM .

Element	**C**	**Si**	**Mn**	**P**	**S**	**Fe**	**CE**
As analyzed using XRF (wt.%)	2.70	2.83	0.58	0.148	0.054	93.34	3.70
As analyzed using EDX (wt.%)	2.59	2.30	0.59	0.23	0.25	93.04	3.40

Before Etching: Figure 2 reveals (a) the optical and (b) the SEM images of the unetched sample with characteristic flake graphite morphologies which is typical of grey cast iron [18].

This confirms that the as-cast bulk sample was slowly cooled such that there was sufficient time for the carbon (graphite) to grow after initial nucleation. Meanwhile figure 3 show different size range of droplets after before etching and one feature common to all is the absence of flake graphite in even the sample with modest undercooling.

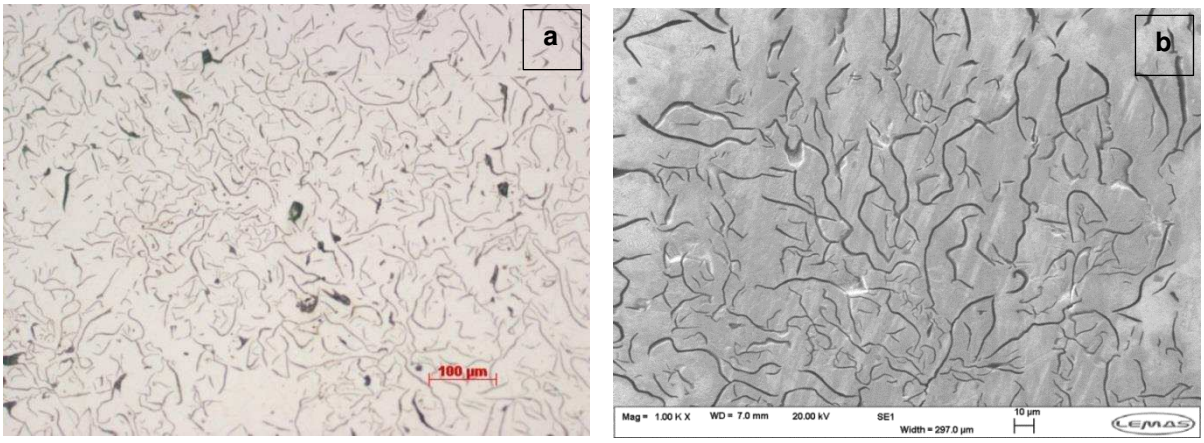

Figure 2: Unetched “as-cast” grey cast iron sample (close to the middle), classified as coarse flake graphite type C in alpha (α)-ferrite matrix.

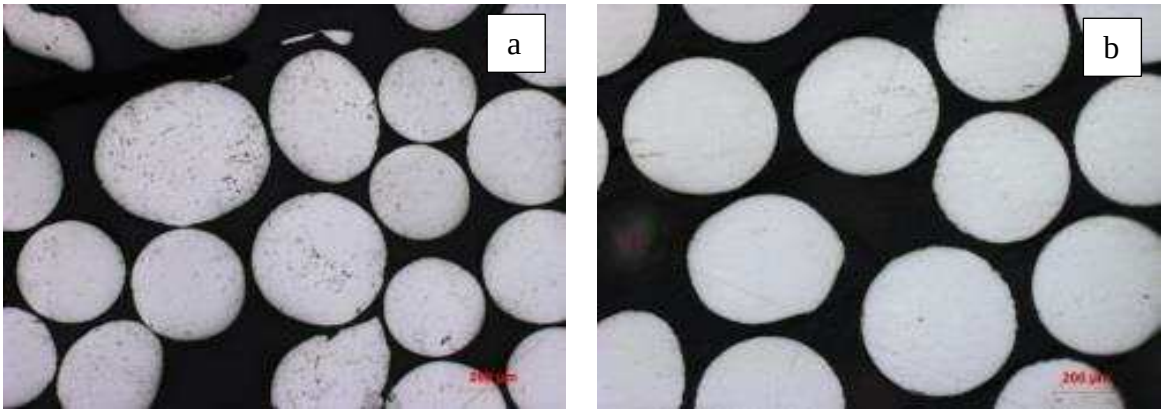

(a) 212 – 300 µm; (b) 300 – 500 µm;

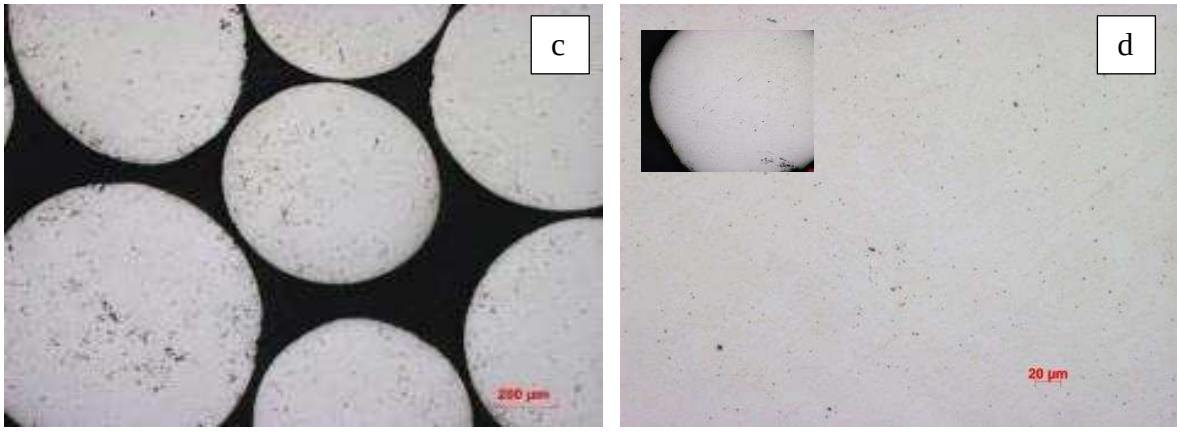

(c) 500 – 800 µm *(d) ≥ 850 µm*

Figure 3: Morphologies of different unetched droplets particles size (a-d) ranges (x 200).

After Etching: Fig. 4 shows the morphologies of the as-cast and the ≥ 850 µm sample etched in 2% nital respectively. This etchant is preferred since it gives better phase contrast as compared to picral or Murakanmi reagent. Two distinct morphologies were revealed in all the droplets which were later identified using x-ray diffraction analysis.

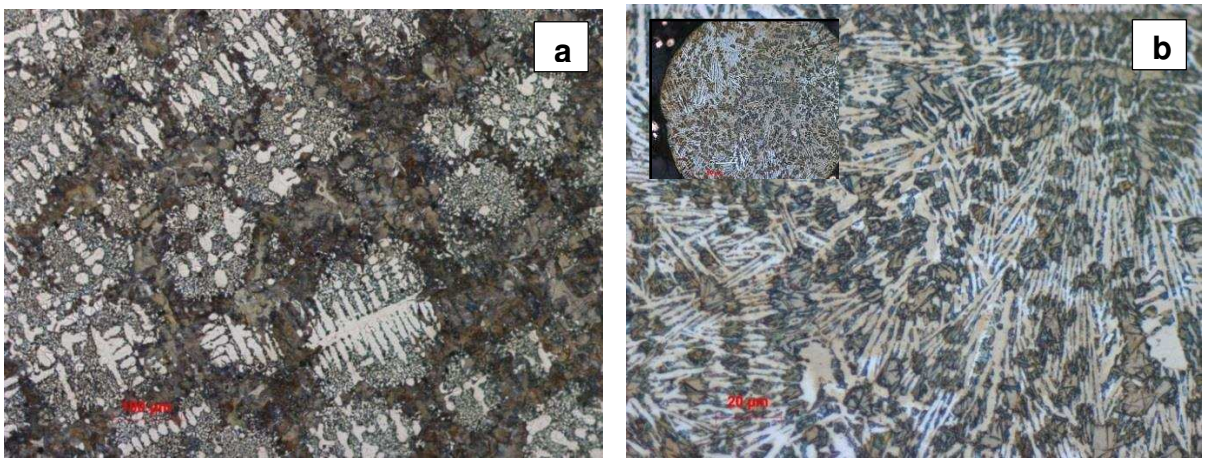

Figure 4: Shows the morphologies of (a) as-cast and (b) ≥ 850 droplet samples. These micrographs reveal the samples dendritic microstructures after etching in 2% Nital; compared to those shown in Fig. x4, they reveal the dendrites (ferrite) in as-cast; (retained austenite) in the droplet samples and the interdendritic phase which is identified as pearlite.

The effect of cooling rate on the evolving microstructures of the different droplets and that of the as-cast sample is as shown in Fig. 5. It reveals the morphologies of the samples with clear evidence of less fragmentation of dendrites as cooling rate increases with particle size reduction. There is traceable consistency of morphological changes with the cooling rate and identified phases which varies in quantities as the droplet size reduction. The distinctiveness of these micrographs confirms the higher cooling rate as particle size reduces. Hence, the cooling rate increases sharply with decreasing droplet diameter for powders under 75 µm with estimated cooling rate of 7.04×10^4 Ks^{-1}.

Morphologies and Phase identification: The dendrites (light section) grow out as a single homogeneous phase is identified as ferrite in the as-cast sample but as austenite in the moderately bigger droplets as indicated in the selected XRD results presented Fig. 6. Meanwhile, the interdendritic (dark section) is made of alternating lamella layers of two different phases identified as cementite and ferrite respectively. Again the identified phases are present in all the droplet samples but in different proportion as indicated in different positions on the XRD graphs. It was observed that as the droplet size reduces (i.e. increase in cooling rate) the amount of ferrite phase reduced considerably while that of the retained austenite increased.

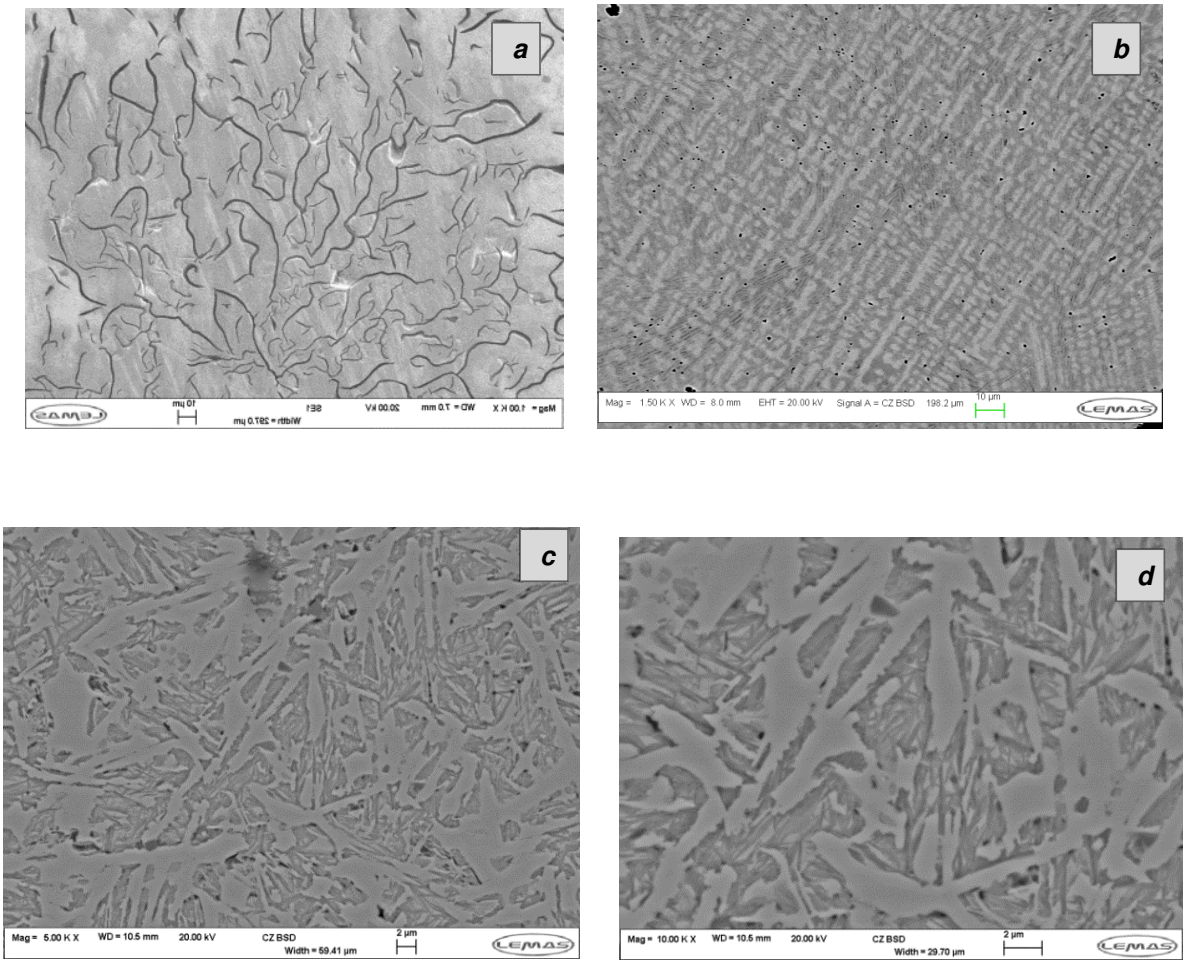

Figure 5: SEM micrographs of samples microstructures at different cooling rate, which increases with decrease in particle sizes especially for the smaller droplets: (a) as-cast sample revealing the flake graphite, (b) 800-500 µm, (c) 106-75 µm and (d) 75-53 µm. The light section is ferrite in the as-cast and retained austenite in the powder particles. The interdendritic section is the pearlite made up of Fe_3C and α-Fe. The dendrites become less fragmented with droplets size reduction. Significant difference was noticed in the morphologies of 106-75 and 75-53 µm sizes which show martensitic microstructure.

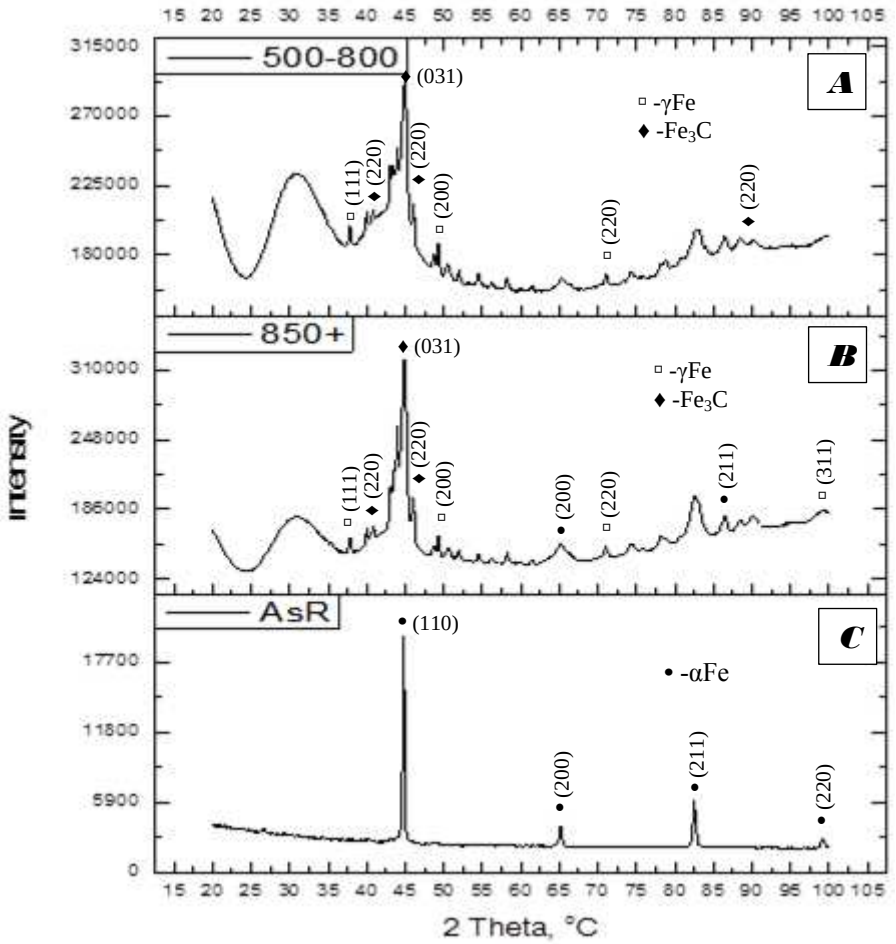

Figure 6: X-ray pattern and phase identification in (A) as-cast, (B) 850+ and (C) 500-800 µm size samples, showing clearly the distinctive features of the these selected samples in terms of morphologies and evolved phases.

Conclusion

Evidences have been presented in this paper by means of metallography and phase analysis on how rapid solidification processing affects the microstructure and mechanical property of commercial grey cast iron even at constant elemental composition. The optical and SEM micrographs obtained in the course of this study along with XRD result showed that the structure of conventionally cooled as-cast low-alloyed commercial grey cast iron is ferritic with well-defined flake graphite network embedded randomly in the iron matrix. This typical microstructure of slowly cooled grey cast iron is found to be adjustable using containerless drop-tube processing technique and the evolved microstructures impact on the mechanical property of the powder particles produced. The droplet sizes are inversely related to the cooling rate ranging from 10^2 Ks^{-1} for conventionally solidified control sample to 7.88 x 10^4 Ks^{-1} for $\leq$ 53 µm diameter size droplets. Hence, increasing the cooling rate resulted in microstructural refinement which translated the effect of processing on structure and property of this very important commercial grey cast iron.

Acknowledgement

This research was carried out in the Institute for Materials Research, University of Leeds. The authors want to thank Dianne Cochrane for metallography, Stuart Micklethwaite and John Harrington of LEMAS, Leeds for their support of electron microscope investigations.

References

[1] L. Battezzati, M. Baricco, S. Curiotto, Acta Materialia 53 (2005) 1849 – 1856.
[2] E.G. Castle, A.M. Mullis, R.F. Cochrane, Acta Materialia 66 (2014) 378 -387.
[3] Liu N, Yang G, Liu F, Chen Y, Yang C, Lu Y, et al. Mater. Charact. 2006;57:115.
[4] J. Gao, B. Wei, J. Alloys Compd. 285 (1999) 229 – 232.
[5] J. Gao, T. Volkmann, S. Reutzel, D.M. Herlach, J. Alloy. Compd. 3880 (2005) 235-240.
[6] F. Gillessen, D.M. Herlarch, Mater. Sci. Eng. 97 (1988) 147 – 151.
[7] C.D. Cao, X.Y. Lu, B. Wei, Adv. Space Res.24 (10) (1999) 1251 – 1255.
[8] A.F. Norman, K. Eckler, A. Zambon, F. Gartner, S.A. Moir, E. Ramous, D.M. Herlach, A.L. Greer, Acta Mater. 46 (10) (1998) 3355-3370.
[9] R.C. Yu, F.X. Zhang, J. Zhang, W.K. Wang, J. Applied Phys. 77, 4334 (1995) 4334-4338
[10] E. Cadirli, D.M. Herlach, T. Volkmann, J. Non-Cryst. Solids 356 (2010) 461-466.
[11] F. Gillessen, Ph.D. Thesis, Ruhr-Universitat Bochum, Germany, 1989.
[12] S. Sugiyama, S. Ozawa, I. Jimbo, S. Hirosawa, K. Kuribayashi, J. Cryst. Growth 275 (2005) e2019-e2024.
[13] L.L. Lacy, M.B. Robinson, T.J. Rathz, J. Cryst. Growth 51 (1981) 47-60.
[14] B. Vinet, L. Cortella, J.J. Favier, P. Derse, Appl. Phys. Lett. 58 (1991) 97.
[15] R.J. Bayuzick, N.D. Evans, W.H. Hofmeister, M.B. Robinson, Microgravity containerless processing in long drop tubes, in: Proceedings of the Symposium on Space Industrialization, Huntsville, AL, 1984.
[16] T.J. Rathz, M.B. W.H. Hofmeister, R.J. Bayuzick, Rev. Sci. Instrum. 61 (1990) 3846.
[17] D.M. Stefanescu, Mater. Sci. Eng. A A413 (2005) 322-333.
[18] M. Cluhan, Metal Handbook 15 (1988) ASM 629-646.